Supporting Information for:

Rapid and Quantitative Measurement of Metabolic Stability without Chromatography or Mass Spectrometry

*Matthew J. Traylor, Jessica D. Ryan, Eric S. Arnon, Jonathan S. Dordick, and Douglas S. Clark**

Contents:

1. Materials and Methods

Materials

The substrates, testosterone, dextromethorphan, amitriptyline, racemic metoprolol, diclofenac, tolbutamide, 3-methylindole, and lidocaine; the inhibitors, 1-aminobenzotriazole and 1-phenylimidazole; the enzymes, catalase from bovine liver and superoxide dismutase from bovine erythrocytes; and nicotinamide adenine dinucleotide phosphate (NADPH) were purchased from Sigma (St. Louis, MO). Microsomes from baculovirus-infected insect cells (Baculosomes) expressing human P450 isoforms and rabbit cytochrome P450 reductase were purchased from Invitrogen (Carlsbad, Ca). Pooled human liver microsomes (catalog number 452161) were purchased from BD Biosciences (Woburn, MA). All chemicals were used as received.

Metabolic stability assay

Metabolic stability assays were prepared in triplicate for each condition tested. CYP3A4 containing Baculosomes were assayed at 25 nM, while all other P450 enzymes were assayed at 50 nM. CYP2C9 was assayed at 50 mM potassium phosphate, while all other P450 enzymes were assayed at 100 mM. Test compounds for CYP2C9 were dissolved in DMSO and added to a final DMSO concentration of 0.5 %, while the test compounds for all other enzymes were dissolved in methanol and added to a final methanol concentration of 1%. CYP1A2 was assayed at pH 8.0, while all other assays were at pH 7.4. Experiments with pooled human liver microsomes were conducted at pH 7.4 in 100 mM potassium phosphate and a final methanol concentration of 1% with an inhibitor concentration of 10 μM 1-phenylimidazole and substrate concentrations of 10 μM dextromethorphan and 100 μM of diclofenac, phenacetin, and testosterone. Inhibition

studies with CYP3A4 containing Baculosomes were conducted in the presence of 100 μM testosterone. Catalase and superoxide dismutase were included in all assays at 100 U/mL and 50 U/mL, respectively. The MitoXpress oxygen probe (Luxcell Biosciences, Cork, Ireland) was reconstituted in deionized water and added to the reactions at a 15-fold dilution per the manufacturer's instructions. NADPH solutions were prepared fresh daily and the concentration was checked via absorbance using a molar extinction coefficient of 6.22 $mM^{-1}cm^{-1}$. Reactions were incubated for 20 min at room temperature before initiation with NADPH to a final concentration of 350 μM and a final volume of 100 μL in a 96-well plate. Directly upon reaction initiation, samples were transferred to a 384-well quartz plate (JNETDirect Biosciences, Herndon, VA) and sealed with aluminum sealing film (catalog number 276014 Nunc, Rochester NY) such that no air bubbles were trapped in the wells. The reactions were followed via fluorescence intensity measurements from the bottom in a Spectramax M5 plate reader (Molecular Devices, Sunnyvale CA) at 25 °C. Fluorescence intensity was simultaneously recorded at two excitation/emission wavelengths: 385 nm/460 nm for NADPH and 380 nm/650 nm for the oxygen probe. Upon completion of data collection, assay wells were visually inspected for the presence of bubbles. If bubbles were found to have been sealed into a well, data from this well was not used.

MitoXpress is a fluorescent, platinum porphyrin that is collisionally quenched by dissolved oxygen. The relationship between probe fluorescence and oxygen concentration follows the well-known Stern-Volmer expression[1]. The Stern-Volmer quenching constant, K_{SV}, was calculated from a two-point oxygen calibration curve on each assay plate consisting of an air-saturated and a deoxygenated standard. The air saturated point

was taken as the average of the initial oxygen signal from the assay wells while the deoxygenated standard was generated enzymatically, consisting of 50 nM CYP3A4, 100 μM testosterone, and 350 μM NADPH. Although the maximum absorbance of NADPH is at 340 nm, fluorescence excitation at 380 nm was chosen to reduce the inner-filter effect and increase standard curve linearity. NADPH standard curves fit well to a second order polynomial ($R^2 > 0.999$). On-plate standards for both oxygen and NADPH were included in each experiment and exhibited good day to day reproducibility (within 10%).

The rates of depletion of NADPH and oxygen were calculated from the linear portion of the time-dependent concentration curves. A pre-steady state lag phase lasting between 10 and 25 minutes was observed with CYP1A2, CYP2C9, and CYP2D6 containing Baculosomes. This lag is attributed to the time required for the pseudo-steady state assumption to become valid (i.e. the time required for the concentrations of hydrogen peroxide and superoxide to reach steady state levels), and this portion of the data was not used in calculating depletion rates.

Chromatography

Chromatographic validation assays were conducted in duplicate at identical assay compositions as the multiwell plate assays, except without the addition of the oxygen probe. The CYP1A2 mediated depletion of lidocaine at 300 μM and 3-methylindole at 500 μM was quantified with gas chromatography. Reactions were stopped at 5 time points with the addition of an equal volume of hexane including internal standard. The organic phase was injected into a 25 m, 250 μm (ID) Varian FactorFour VF-5ms capillary column installed in a Varian 3900 gas chromatograph with an FID detector (Walnut Creek, CA). The injector and detector temperatures were 250 and 280 °C,

respectively. The samples were injected at a split ratio of 20, with helium as the carrier gas at a flowrate of 2.0 mL/min. The column temperature was maintained at 60 °C for 2 min, ramped to 120 °C at a rate of 10 °C/min, and finally ramped to 250 °C at a rate of 45 °C/min, which was held for 5 min. The CYP2D6 mediated depletion of amitriptyline at 60 μM and metoprolol at 100 μM were quantified with high performance liquid chromatography (HPLC). Reactions were quenched at 4 time points with 100 uL of ice-cold methanol containing internal standard. Samples were analyzed on a 1200 series Agilent HPLC with a reverse-phase Alltech Prevail C18 3 μm 3.0x150 mm column with a 0.4 ml/min flow rate and a gradient of 40 – 90% methanol over 13 min with a constant 0.05% concentration of formic acid.

2. Derivation of Rate Equations for P450 Systems

Kinetic analysis of the cytochrome P450 system

$$RH + O_2 + NADPH + H^+ \rightarrow ROH + NADP^+ + H_2O \quad (1)$$

$$O_2 + NADPH + H^+ \rightarrow H_2O_2 + NADP^+ \quad (2)$$

$$O_2 + 2NADPH + 2H^+ \rightarrow 2H_2O + 2NADP^+ \quad (3)$$

$$O_2 + \frac{1}{2}NADPH \rightarrow O_2^{\bullet -} + \frac{1}{2}NADP^+ + \frac{1}{2}H^+ \quad (4)$$

Overall Reaction Rates

Reaction 1 : $-r_{1RH} = -r_{1O_2} = -r_{1NADPH} = r_{1ROH}$

Reaction 2 : $-r_{2O_2} = -r_{2NADPH} = r_{2H_2O_2}$

Reaction 3 : $-r_{3O_2} = -\frac{1}{2} r_{3NADPH}$

Reaction 4 : $-r_{4O_2} = -2r_{4NADPH} = r_{4O_2^{\bullet -}}$

Net Rates

$$r_{O_2} = r_{1O_2} + r_{2O_2} + r_{3O_2} + r_{4O_2}$$

$$r_{NADPH} = r_{1NADPH} + r_{2NADPH} + r_{3NADPH} + r_{4NADPH}$$

$$r_{H_2O_2} = r_{2H_2O_2}$$

$$r_{O_2^{\bullet -}} = r_{4O_2^{\bullet -}}$$

From Net Rates

$$-r_{3O_2} = -r_{O_2} + r_{1O_2} + r_{2O_2} + r_{4O_2}$$

$$-\frac{1}{2} r_{3NADPH} = -\frac{1}{2} r_{NADPH} + \frac{1}{2} r_{1NADPH} + \frac{1}{2} r_{2NADPH} + \frac{1}{2} r_{4NADPH}$$

Equating the two

$$-r_{O_2} + r_{1O_2} + r_{2O_2} + r_{4O_2} = -\frac{1}{2} r_{NADPH} + \frac{1}{2} r_{1NADPH} + \frac{1}{2} r_{2NADPH} + \frac{1}{2} r_{4NADPH}$$

Where

$$r_{1O_2} = r_{1RH} = r_{1NADPH}$$

$$r_{2O_2} = r_{2NADPH} = -r_{2H_2O_2} = -r_{H_2O_2}$$

$$r_{4O_2} = -r_{4O_2^{\bullet -}} = -r_{O_2^{\bullet -}} + r_{5O_2^{\bullet -}} = -r_{O_2^{\bullet -}}$$

$$r_{4NADPH} = -\frac{1}{2} r_{4O_2^{\bullet -}} = -\frac{1}{2} r_{O_2^{\bullet -}}$$

Thus

$$-r_{O_2} + r_{RH} - r_{H_2O_2} - r_{O_2^{\bullet -}} = -\frac{1}{2} r_{NADPH} + \frac{1}{2} r_{RH} - r_{H_2O_2} - \frac{1}{2} r_{O_2^{\bullet -}}$$

Solve for $-r_{RH}$, where each value in parenthesis is a positive quantity

$$\left(-r_{RH}\right) = 2\left(-r_{O_2}\right) - \left(-r_{NADPH}\right) - \left(r_{H_2O_2}\right) - \left(r_{O_2^{\bullet -}}\right)$$

Kinetic analysis of the cytochrome P450 system with the addition of superoxide dismutase (rxn 5) and catalase (rxn 6)

$$RH + O_2 + NADPH + H^+ \rightarrow ROH + NADP^+ + H_2O \quad (1)$$

$$O_2 + NADPH + H^+ \rightarrow H_2O_2 + NADP^+ \quad (2)$$

$$O_2 + 2NADPH + 2H^+ \rightarrow 2H_2O + 2NADP^+ \quad (3)$$

$$O_2 + \frac{1}{2}NADPH \rightarrow O_2^{\bullet -} + \frac{1}{2}NADP^+ + \frac{1}{2}H^+ \quad (4)$$

$$2O_2^{\bullet -} + 2H^+ \rightarrow O_2 + H_2O_2 \quad (5)$$

$$2H_2O_2 \rightarrow O_2 + 2H_2O \quad (6)$$

Overall Reaction Rates

Reaction 1 : $-r_{1RH} = -r_{1O_2} = -r_{1NADPH} = r_{1ROH}$

Reaction 2 : $-r_{2O_2} = -r_{2NADPH} = r_{2H_2O_2}$

Reaction 3 : $-r_{3O_2} = -\frac{1}{2} r_{3NADPH}$

Reaction 4 : $-r_{4O_2} = -2r_{4NADPH} = r_{4O_2^{\bullet -}}$

Reaction 5 : $-\frac{1}{2} r_{5O_2^{\bullet -}} = r_{5O_2} = r_{5H_2O_2}$

Reaction 6 : $-\frac{1}{2} r_{6H_2O_2} = r_{6O_2}$

Net Rates

$r_{O_2} = r_{1O_2} + r_{2O_2} + r_{3O_2} + r_{4O_2} + r_{5O_2} + r_{6O_2}$

$r_{NADPH} = r_{1NADPH} + r_{2NADPH} + r_{3NADPH} + r_{4NADPH}$

$r_{H_2O_2} = r_{2H_2O_2} + r_{5H_2O_2} + r_{6H_2O_2}$

$r_{O_2^{\bullet -}} = r_{4O_2^{\bullet -}} + r_{5O_2^{\bullet -}}$

From Net Rates

$-r_{3O_2} = -r_{O_2} + r_{1O_2} + r_{2O_2} + r_{4O_2} + r_{5O_2} + r_{6O_2}$

$-\frac{1}{2} r_{3NADPH} = -\frac{1}{2} r_{NADPH} + \frac{1}{2} r_{1NADPH} + \frac{1}{2} r_{2NADPH} + \frac{1}{2} r_{4NADPH}$

Equating the two

$-r_{O_2} + r_{1O_2} + r_{2O_2} + r_{4O_2} + r_{5O_2} + r_{6O_2} = -\frac{1}{2} r_{NADPH} + \frac{1}{2} r_{1NADPH} + \frac{1}{2} r_{2NADPH} + \frac{1}{2} r_{4NADPH}$

Where

$$r_{1O_2} = r_{1RH} = r_{1NADPH}$$

$$r_{2O_2} = r_{2NADPH} = -r_{2H_2O_2} = -r_{H_2O_2} + r_{5H_2O_2} + r_{6H_2O_2}$$

$$r_{4O_2} = -r_{4O_2^{\bullet-}} = -r_{O_2^{\bullet-}} + r_{5O_2^{\bullet-}} = -r_{O_2^{\bullet-}} - 2r_{5H_2O_2}$$

$$r_{5O_2} = r_{5H_2O_2}$$

$$r_{6O_2} = -\frac{1}{2} r_{6H_2O_2}$$

$$r_{4NADPH} = -\frac{1}{2} r_{4O_2^{\bullet-}} = -\frac{1}{2} r_{O_2^{\bullet-}} - r_{5H_2O_2}$$

Thus

$$-r_{O_2} + r_{RH} + \left[-r_{H_2O_2} + r_{5H_2O_2} + r_{6H_2O_2}\right] + \left[-r_{O_2^{\bullet-}} - 2r_{5H_2O_2}\right] + r_{5H_2O_2} - \frac{1}{2} r_{6H_2O_2} =$$

$$-\frac{1}{2} r_{NADPH} + \frac{1}{2} r_{RH} + \frac{1}{2}\left[-r_{H_2O_2} + r_{5H_2O_2} + r_{6H_2O_2}\right] + \frac{1}{2}\left[-\frac{1}{2} r_{O_2^{\bullet-}} - r_{5H_2O_2}\right]$$

Solve for $-r_{RH}$, where each value in parenthesis is a positive quantity

$$(-r_{RH}) = 2(-r_{O_2}) - (-r_{NADPH}) - (r_{H_2O_2}) - \frac{2}{3}(r_{O_2^{\bullet-}})$$

A pseudo - steady state assumption on H_2O_2 and $O_2^{\bullet-}$ assumes that the rate of change of the concentration of an intermediate $(r_{H_2O_2}$ and $r_{O_2^{\bullet-}})$ is much less than that of the reactants or products $(r_{RH}, r_{O_2}$, and $r_{NADPH})$:

$$|r_{H_2O_2}| \ll |r_{NADPH}|, |r_{O_2}|, \text{and} |r_{RH}|$$

$$|r_{O_2^{\bullet-}}| \ll |r_{NADPH}|, |r_{O_2}|, \text{and} |r_{RH}|$$

This assumption is made based on the inclusion of superoxide dismutase (rxn 5) and catalase (rxn 6), which ensure that H_2O_2 and $O_2^{\bullet-}$ do not accumulate in the assay, thus the overall rate equation can be simplified to the final form :

$$(-r_{RH}) = 2(-r_{O_2}) - (-r_{NADPH})$$

3. Supporting Figures

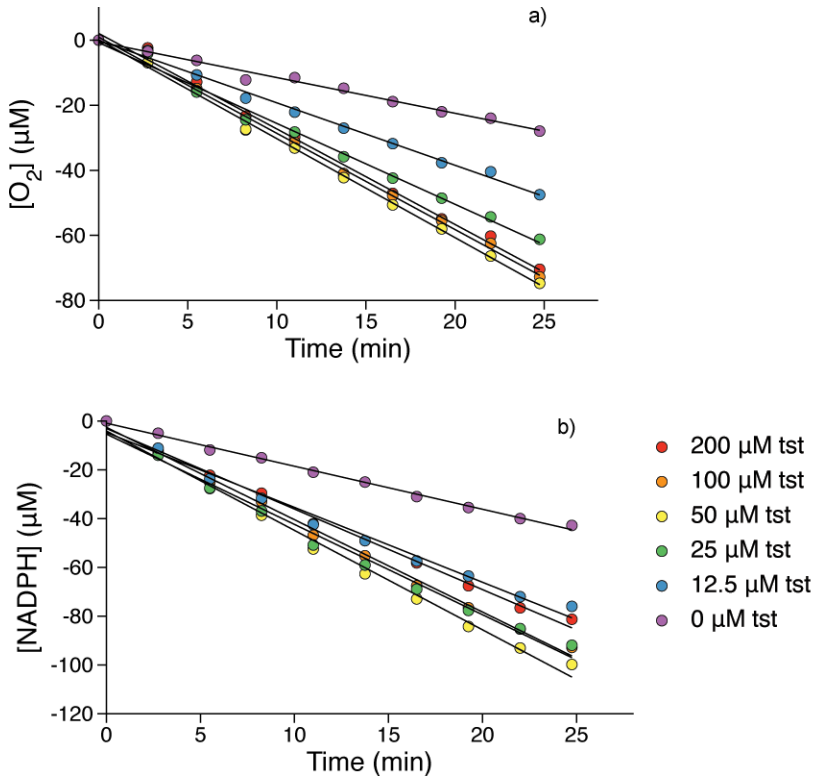

Figure S1. Depletion of (a) oxygen and (b) NADPH in the CYP3A4 oxidation of testosterone.

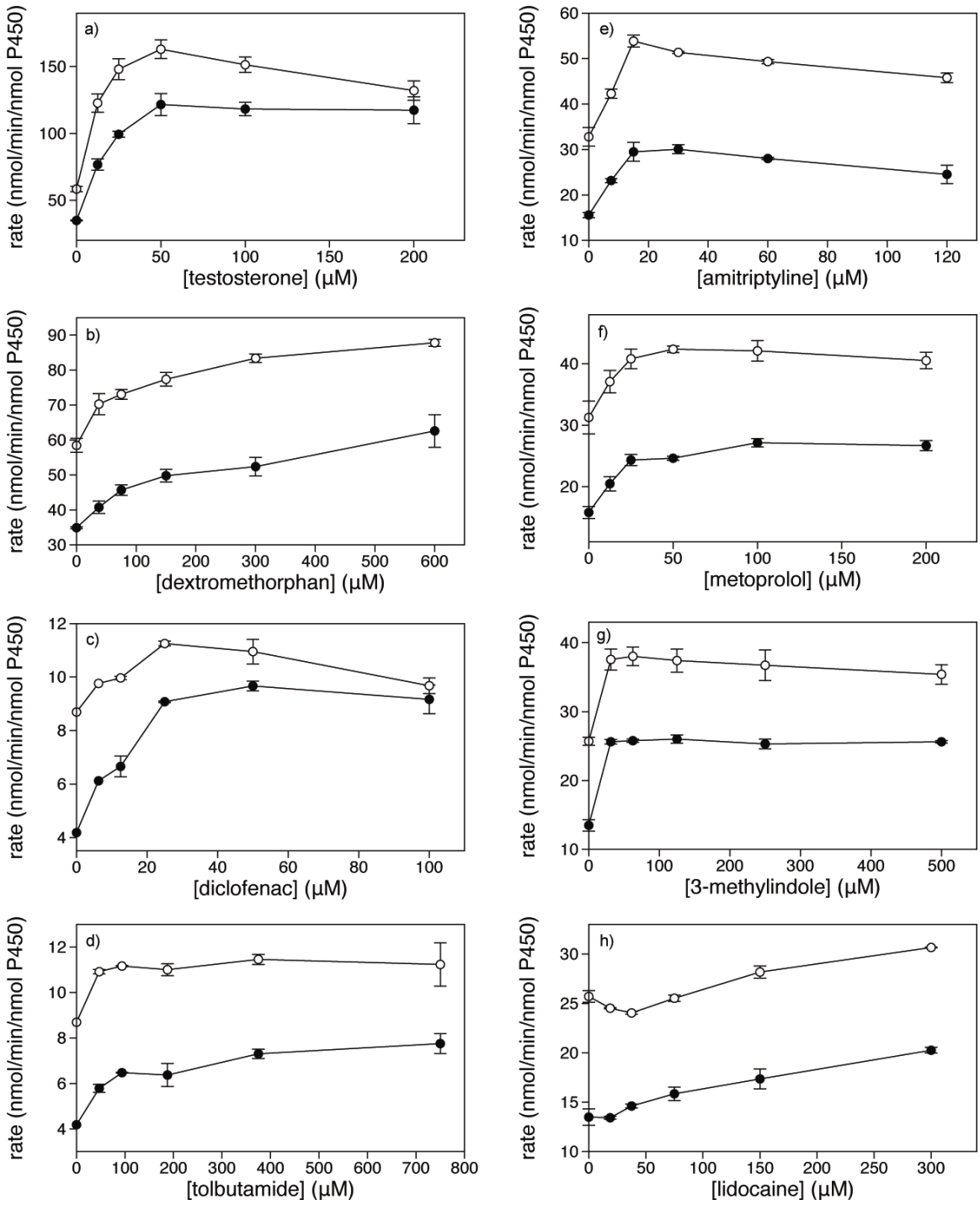

Figure S2. Measured rates of depletion of (○) NADPH and (●) oxygen in the CYP3A4 oxidation of (a) testosterone and (b) dextromethorphan, the CYP2C9 oxidation of (c) diclofenac and (d) tolbutamide, the CYP2D6 oxidation of (e) amitriptyline and (f) metoprolol, and the CYP1A2 oxidation of (g) 3-methylindole and (h) lidocaine.

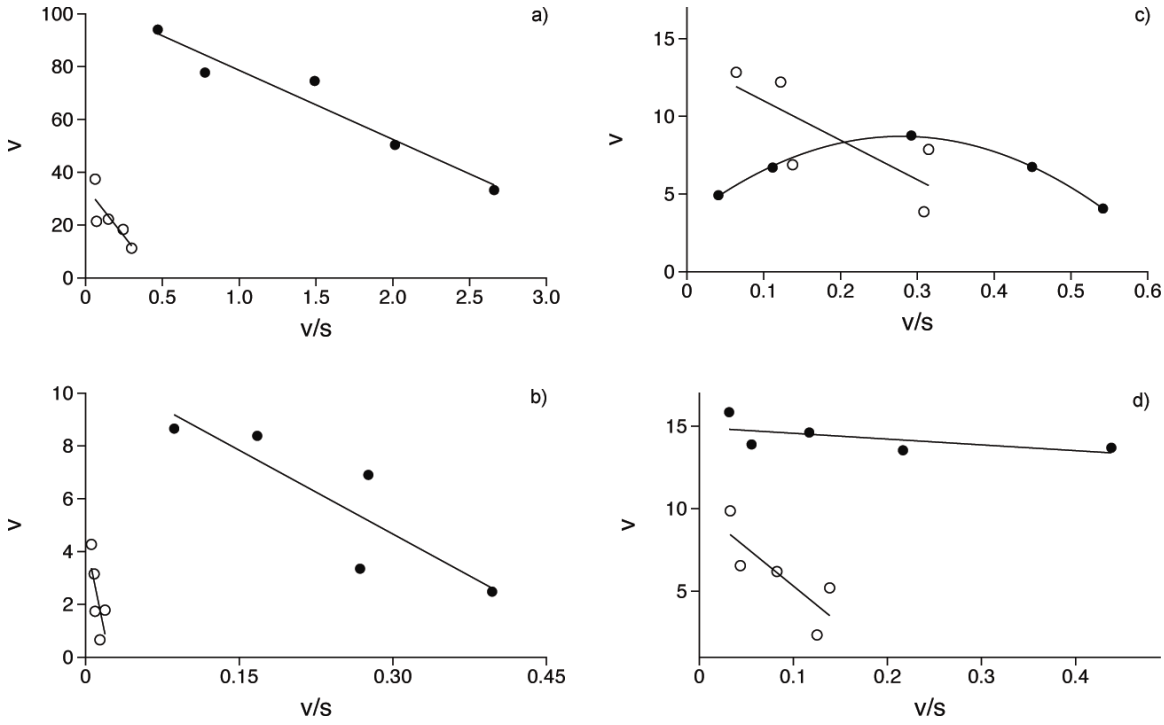

Figure S3. Eadie-Hofstee plots of (a) CYP3A4 oxidation of (●) testoterone and (○) dextromethorphan; (b) CYP2C9 oxidation of (●) diclofenac and (○) tolbutamide; (c) CYP2D6 oxidation of (●) amitriptyline and (○) metoprolol; and (d) CYP1A2 oxidation of (●) 3-methylindole and (○) lidocaine. Data for CYP2D6 oxidation of amitriptyline were fit to substrate inhibition kinetics.

4. Calculation of Literature Metabolic Stabilities for Systems with Multiple Products

For P450 catalyzed reactions that generate multiple products, the measured metabolic stability is equal to the sum of the rates of generation of each product. Literature values for the catalytic constants of substrate depletion were calculated from the reported values for the generation of each of the products. The rate of generation of each product was summed to find the total depletion of substrate. This data was fit to the Eadie-Hofstee linearized form of the Michaelis-Menten equation, from which kinetic constants were extracted.

CYP3A4 Oxidation of Testosterone

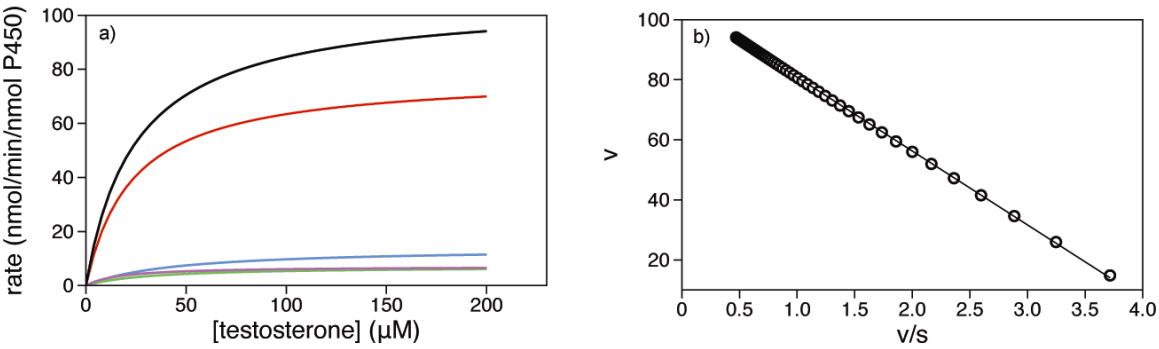

Figure S4. Modeling the rate of substrate depletion in the CYP3A4 oxidation of testosterone with (a) the black curve representing the sum of the rate of generation of the major product species, each of which is shown with a colored curve, and (b) the Eadie-Hofstee plot of testosterone depletion from which catalytic constants were extracted.

Table S1. Literature values of the catalytic constants for the major products of the CYP3A4 oxidation of testosterone[2] and the calculated catalytic constants for testosterone depletion.

	6β-hydroxylation	2β-hydroxylation	15β-hydroxylation	1β-hydroxylation	Total
k_{cat} (min^{-1})	78	14	7.1	7.1	105.4
K_M (μM)	23	44	32	17	24.6

CYP3A4 Oxidation of Dextromethorphan

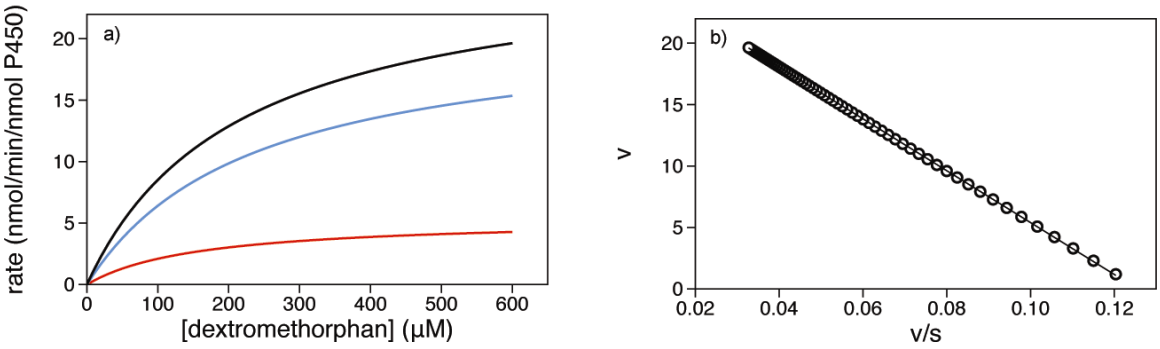

Figure S5. Modeling the rate of substrate depletion in the CYP3A4 oxidation of dextromethorphan with (a) the black curve representing the sum of the rate of generation of the major product species, each of which is shown with a colored curve, and (b) the Eadie-Hofstee plot of dextromethorphan depletion from which catalytic constants were extracted.

Table S2. Literature values of the catalytic constants for the major products of the CYP3A4 oxidation of dextromethorphan[3] and the calculated catalytic constants for dextromethorphan depletion.

	O-demethylation	N-demethylation	Total
k_{cat} (min^{-1})	5.4	21.3	26.5
K_M (μM)	157	232	210.4

5. Analysis of the Optical Properties of the Top 30 Bestselling Drugs

A test compound is expected to interfere with the MesaPlate if the compound is absorbent or fluorescent in the range of NADPH or the MitoXpress O_2 probe. However, such interference should be resolvable using common methods of spectral unmixing.

Table S3. Expected optical interference of top 30 bestselling drugs[4] with the MesaPlate.

Rank	Drug	Type	Expected Interference
1	Lipitor	Small molecule	No[5]
2	Nexium	Small molecule	No[6]
3	Plavix	Small molecule	No[7]
4	Advair Diskus	Small molecule	No[8]
5	Seroquel	Small molecule	No[9]
6	Abilify	Small molecule	No[10]
7	**Singulair**	**Small molecule**	**Yes[11]**
8	Actos	Small molecule	No[12]
9	Enbrel	Protein	N/A
10	Epogen	Protein	N/A
11	Remicade	Protein	N/A
12	Crestor	Small molecule	No[13]
13	Avastin	Protein	N/A
14	Neulasta	Protein	N/A
15	OxyContin	Small molecule	No[14]
16	Cymbalta	Small molecule	No[15]
17	Effexor XR	Small molecule	No[16]
18	Lexapro	Small molecule	No[17]
19	Lovenox	Polysaccharide	N/A

20	Zyprexa	Small molecule	No[18]
21	Rituxan	Protein	N/A
22	Humira	Protein	N/A
23	Prevacid	Small molecule	No[19]
24	Aricept	Small molecule	No[20]
25	Flomax	Small molecule	No[21]
26	Valtrex	Small molecule	No[22]
27	Lantus	Protein	N/A
28	Atripla	Small molecule	No[23]
29	Celebrex	Small molecule	No[24]
30	Diovan	Small molecule	No[25]

Table S4. Summary of data in Table S.3.

	Count	Percentage of Small Molecules
Expected Interference	1	4.8 % (1 / 21)
No Expected Interference	20	95.2 % (20 / 21)
N/A (protein, polysaccharide)	9	

6. References

Full citation of reference 2 from the manuscript

(2) Bjornsson, T. D.; Callaghan, J. T.; Einolf, H. J.; Fischer, V.; Gan, L.; Grimm, S.; Kao, J.; King, S. P.; Miwa, G.; Ni, L.; Kumar, G.; McLeod, J.; Obach, R. S.; Roberts, S.; Roe, A.; Shah, A.; Snikeris, F.; Sullivan, J. T.; Tweedie, D.; Vega, J. M.; Walsh, J.; Wrighton, S. A. *Drug Metab. Dispos.* **2003**, *31*, 815

References for the Supporting Information

(1) O'donovan, C.; Hynes, J.; Yashunski, D.; Papkovsky, D. B. *Journal of Materials Chemistry* **2005**, *15*, 2946.

(2) Krauser, J. A.; Guengerich, F. P. *J Biol Chem* **2005**, *280*, 19496.

(3) Yu, A. M.; Haining, R. L. *Drug Metab Dispos* **2001**, *29*, 1514.

(4) Bartholow, M. *Pharmacy Times* **2010**, *10*.

(5) Alarcon, E.; Gonzalez-Bejar, M.; Gorelsky, S.; Ebensperger, R.; Lopez-Alarcon, C.; Netto-Ferreira, J. C.; Scaiano, J. C. *Photoch Photobio Sci* **2010**, *9*, 1378.

(6) Yang, R.; Schulman, S. G.; Zavala, P. J. *Anal Chim Acta* **2003**, *481*, 155.

(7) Zaazaa, H. E.; Abbas, S. S.; Abdelkawy, M.; Abdelrahman, M. M. *Talanta* **2009**, *78*, 874.

(8) Michael, Y.; Chowdhry, B. Z.; Ashurst, I. C.; Snowden, M. J.; Davies-Cutting, C.; Gray, S. *Int J Pharm* **2000**, *200*, 279.

(9) Mandrioli, R.; Fanali, S.; Ferranti, A.; Raggi, M. A. *J Pharmaceut Biomed* **2002**, *30*, 969.

(10) Kalaichelvi, R.; Thangabalan, B.; Rao, D. S.; Jayachandran, E. *E-J Chem* **2009**, *6*, S87.

(11) Meras, I. D.; Espinosa-Mansilla, A.; Rodriguez, D. A. *J Pharmaceut Biomed* **2007**, *43*, 1025.

(12) (a) Hegazy, M. A.; El-Ghobashy, M. R.; Yehia, A. M.; Mostafa, A. A. *Drug Test Anal* **2009**, *1*, 339, (b) Radhakrishna, T.; Rao, D. S.; Reddy, G. O. *J Pharmaceut Biomed* **2002**, *29*, 593.

(13) Gupta, A.; Mishra, P.; Shah, K. *E-J Chem* **2009**, *6*, 89.

(14) Brogle, K.; Ornaf, R. M.; Wu, D.; Palermo, P. J. *J Pharmaceut Biomed* **1999**, *19*, 669.

(15) Liu, X. P.; Du, Y. X.; Wu, X. L. *Spectrochim Acta A* **2008**, *71*, 915.

(16) (a) Matoga, M.; Pehourcq, F.; Titier, K.; Dumora, F.; Jarry, C. *Journal of Chromatography B* **2001**, *760*, 213, (b) Purdel, N. C.; Balalau, D.; Ilie, M.; Arama, C. C. *Farmacia* **2010**, *58*, 62.

(17) Taha, E. A.; Salama, N. N.; Wang, S. *Anal Chem Insights* **2009**, *4*, 1.

(18) Shevchenko, V. P.; Nagaev, I. Y.; Kost, N. V.; Ivanov, I. A.; Myasoedov, N. F. *Dokl Chem* **2010**, *434*, 260.

(19) Rahman, N.; Bano, Z.; Azmi, S. N. H.; Kashif, M. *J Serb Chem Soc* **2006**, *71*, 1107.

(20) *Donepezil*; Asiri, Y. A.; Mostafa, G. A. E., Eds.; Elsevier, 2010; Vol. 35.

(21) Nanda, R. K.; Gaikwad, J.; Prakash, A. *Asian Journal of Research Chemistry* **2009**, *2*, 63.

(22) Ganesh, M.; Narasimharao, C. V.; Kumar, A. S.; Kamalakannan, K.; Vinoba, M.; Mahajan, H. S.; Sivakumar, T. *E-J Chem* **2009**, *6*, 814.

(23) (a) Sudha, T.; Saminathan, J.; Hemalatha, P. V.; Ravikumar, V. R. *Int J Pharm* **2010**, *1*, 26, (b) Shown, I.; Banerjee, S.; Ramchandran, A. V.; Geckeler, K. E.; Murthy, C. N. *Macromolecular Symposia* **2010**, *287*, 51, (c) Kumar, Y. A.; Rao, N. R. *E-J Chem* **2010**, *7*, 856.

(24) (a) Bebawy, L. I.; Moustafa, A. A.; Abo-Talib, N. F. *J Pharmaceut Biomed* **2002**, *27*, 779, (b) Damiani, P.; Bearzotti, M.; Cabezon, M. A. *Anal Bioanal Chem* **2003**, *376*, 1141, (c) Starek, M.; Rejdych, M. *Jpc-J Planar Chromat* **2009**, *22*, 399.

(25) Chaudary, A. B.; Patel, R. K.; Chaudary, S. A.; Gadhvi, K. V. *International Journal of Applied Biology and Pharmaceutical Technology* **2010**, *1*, 455.